

CFD of Oscillating Airfoil Pitch Cycle by using PISO Algorithm

Muhammad Amjad Sohail ,Rizwan Ullah

Abstract—This research paper presents the CFD analysis of oscillating airfoil during pitch cycle. Unsteady subsonic flow is simulated for pitching airfoil at Mach number 0.283 and Reynolds number 3.45 millions. Turbulent effects are also considered for this study by using K- ω SST turbulent model. Two-dimensional unsteady compressible Navier-Stokes code including two-equation turbulence model and PISO pressure velocity coupling is used. Pressure based implicit solver with first order implicit unsteady formulation is used. The simulated pitch cycle results are compared with the available experimental data. The results have a good agreement with the experimental data. Aerodynamic characteristics during pitch cycles have been studied and validated.

Keywords—Angle of attack, Centre of pressure, subsonic flow, pitching moment coefficient, turbulence mode

I. INTRODUCTION

THE dynamic stall refers to delay of stall to a higher incidence angle compared with that of the steady state. A main reason is that as an airfoil pitches up, dynamic stall vortex starts on the leading edge of airfoil, develops and subsequently sheds. It is a complex fluid dynamics phenomenon of practical importance and occurs on retreating helicopter rotor blades, rapidly maneuvering aircraft, fluttering compressor blades, and wind turbines. In many cases, dynamic stall becomes primary limiting factor in the performance of the associated vehicle or structure.

Unsteady flows are encountered in many aerospace applications and prediction of unsteady air loads plays a vital role in aircraft and helicopter design [1-3]. Since wind tunnel testing of unsteady flow situations is difficult and expensive, computational studies of wing stall, dynamic stall, blade-vortex interaction of helicopter rotors and aeroelastic problems like flutter, buffeting and gust- response etc., can provide important design data. Flying birds usually flap their wings to generate both lift and thrust. Flapping motion of birds has a coupled pitching and plunging oscillation with some phase difference between them. Recent experimental and computational studies investigated the kinematics, dynamics, flow characteristics of flapping wings and shed some light on the lift, drag, and propulsive power considerations [4, 5]. Yang et al. [6] have computed a sinusoidally pitching and plunging NACA 0012 aerofoil in a uniform stream of low speeds for different motion parameters by using inviscid version of a three-dimensional unsteady compressible

Euler/Navier-Stokes flow solver and optimized for high propulsive efficiency and for high time-averaged thrust coefficient. Theodorsen [7] has developed compact expressions for forces and moments of a flapping plate aerofoil for small perturbed inviscid and incompressible flow. In the prediction of unsteady pressure distributions over aerofoils, the steady-state Kutta-Joukowski condition is assumed. The flow is treated in two classes: the non circulating flow due to the aerofoil vertical acceleration and the circulatory flow due to the wake vortices. Many important features of flapping aerofoil behavior are depicted by the classical linear theory. The thrust force experienced by the flapping aerofoil was given by Garrick [8]. Tuncer and Platzer [9] used a compressible Navier-Stokes solver to compute the unsteady turbulent flow fields and obtained high propulsive efficiency when the flow remains mostly attached over the aerofoil oscillated in plunge and pitch. Isogai et al. [10] performed Navier-Stokes simulations of flow over a NACA 0012 aerofoil undergoing combined pitching and plunging motion at $Re = 105$. Ramamurti and Sandberg [11] performed numerical simulation of the flow over a flapping NACA 0012 aerofoil using a finite element incompressible Navier-Stokes solver at a Reynolds number of 1100. They found that the critical parameter which affects the thrust generation is kh rather than k . They also found that maximum thrust is obtained when the pitching motion leads the plunging motion by 120° and the maximum propulsive efficiency occurs at $\theta = 90^\circ$. Anderson et al. [12] measured the time-averaged thrust coefficient, input power coefficient, and propulsion efficiency of a NACA 0012 aerofoil undergoing combined sinusoidal plunging and pitching motion in the testing tank facility at MIT. K. Siva Kumar uses the Implicit RANS solver for obtaining time-accurate solutions is based on a finite volume nodal point spatial discretization scheme with dual time stepping. The aim is to validate the unsteady solver for flapping motion of the aerofoil. Unsteady flows are encountered in many aerospace applications and prediction of unsteady air loads plays a vital [13]. In the current study Implicit solver is used with PISO pressure velocity coupling algorithm is used to obtain the drag, lift and pitching moment coefficients by using turbulence modeling.

II. MESH GENERATION

The algebraic method is used to generate two-dimensional boundary-fitted grids for NACA0012 airfoil. The height of the first grid next to the body is controlled, and the grids near to the body are normalized to achieve y^+ less than 1. The H-H and C-type boundary- fitted grids are generated at first in order to simulate the aerodynamic forces accurately.

Muhammad Amjad Sohail is PhD student from Beijing University of Aeronautics and Astronautics Beijing China (phone: 0086-13120491221; e-mail: masohailamer@yahoo.com).

Rizwan ullah is PhD student from Nanjing University of Aeronautics and Astronautics Nanjing China (phone: 0086-13120491221; e-mail: rizwanul@yahoo.com).

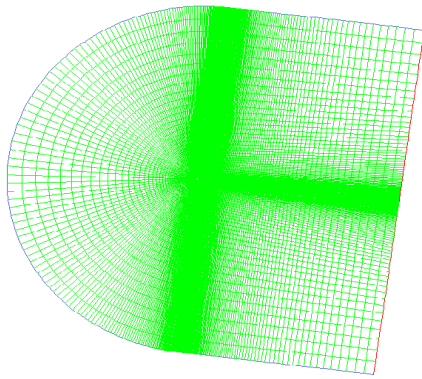


Fig. 1 Generation of mesh around NACA0012 airfoil

III. GOVERNING EQUATIONS AND TURBULENCE MODELS

A. Governing Equations

The system of governing equations for a single-component fluid, written to describe the mean flow properties, is cast in integral Cartesian form for an arbitrary control volume V with differential surface area dA as follows:

$$\frac{\partial}{\partial t} \int_V W dV + \oint [F - G] \cdot dA = \int_V H dV \quad (1)$$

Where the vectors W , F and G are defined as:

$$W = \begin{bmatrix} \rho \\ \rho u \\ \rho v \\ \rho w \\ \rho E \end{bmatrix}, F = \begin{bmatrix} \rho u \\ \rho v u + P \hat{i} \\ \rho v v + P \hat{j} \\ \rho v w + P \hat{k} \\ \rho v E + P v \end{bmatrix}, G = \begin{bmatrix} 0 \\ \tau_{xi} \\ \tau_{yi} \\ \tau_{zi} \\ \tau_{ij} v_j + q \end{bmatrix}$$

Vector H contains source terms such as body forces and energy sources.

Here ρ , v , E , and p are the density, velocity, total energy per unit mass, and pressure of the fluid, respectively. T is the viscous stress tensor, and q is the heat flux.

Total energy E is related to the total enthalpy H by

$$E = H - p / \rho \quad (2)$$

$$\text{Where } H = h + \frac{|v|^2}{2}$$

B. Turbulence Model

To calculate the turbulent flows the $K-\omega$ SST turbulent model is used here.

$$\frac{\partial}{\partial t} (\rho k) + \frac{\partial}{\partial x_i} (\rho k u_i) = \frac{\partial}{\partial x_j} (\Gamma_k \frac{\partial k}{\partial x_j}) + \tilde{G}_k - Y_k + D_k + S_k \quad (3)$$

$$\frac{\partial}{\partial t} (\rho \omega) + \frac{\partial}{\partial x_i} (\rho \omega u_i) = \frac{\partial}{\partial x_j} (\Gamma_\omega \frac{\partial \omega}{\partial x_j}) + G_\omega - Y_\omega + D_\omega + S_\omega \quad (4)$$

C. The PISO Algorithm

The steady-state SIMPLE algorithm can be extended in a straightforward manner for unsteady flows by including the unsteady terms in the Navier-Stokes equations Ref [14]. However, this approach is computationally expensive since several iterations have to be conducted at each timestep.

D. Dual Time Formulation

The implicit-time stepping method (also known as dual-time formulation) is used here for the calculation of detached eddy simulation in the implicit formulation. Density based implicit solver is used for both RANS and LES simulations with SA and $K-\omega$ SST turbulence modeling. Preconditioned pseudo-time-derivative term is used here

$$\frac{\partial}{\partial t} \int_V W dV + \Gamma \frac{\partial}{\partial \tau} \int_V Q dV + \oint [F - G] \cdot dA = \int_V H dV \quad (5)$$

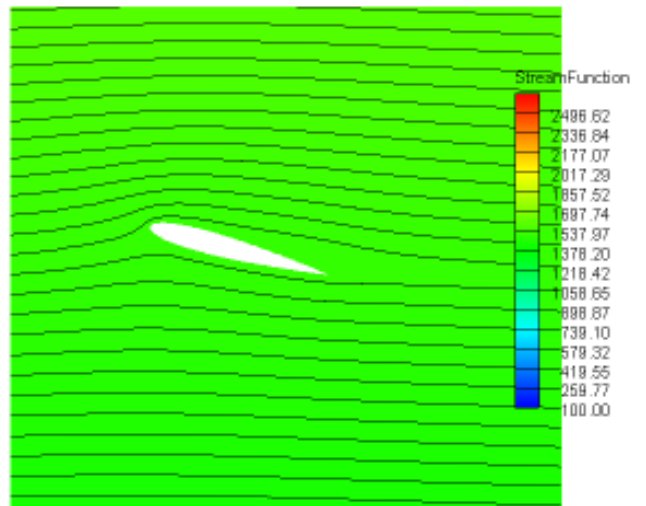
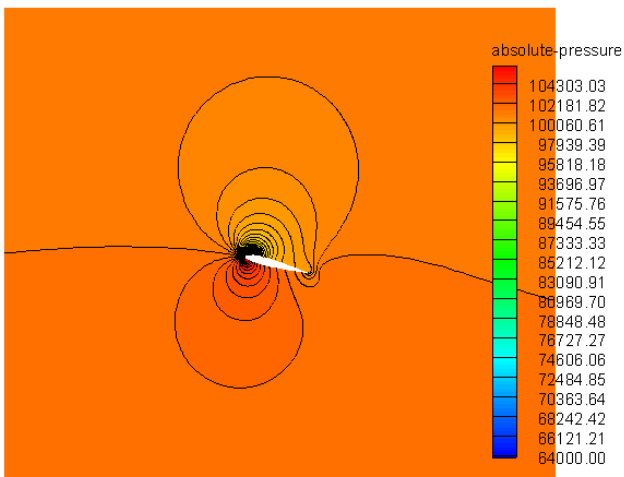
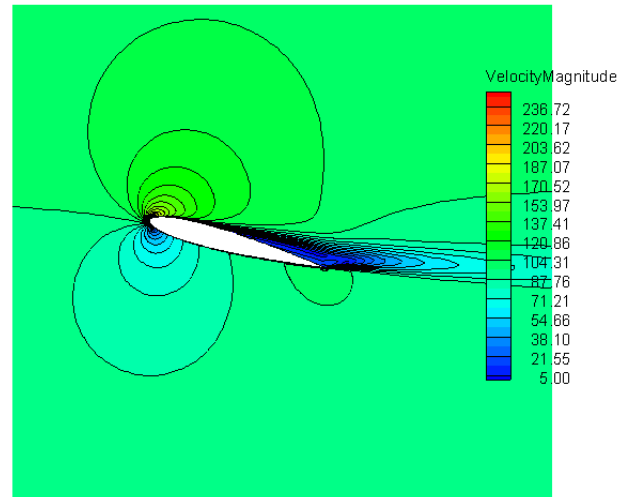
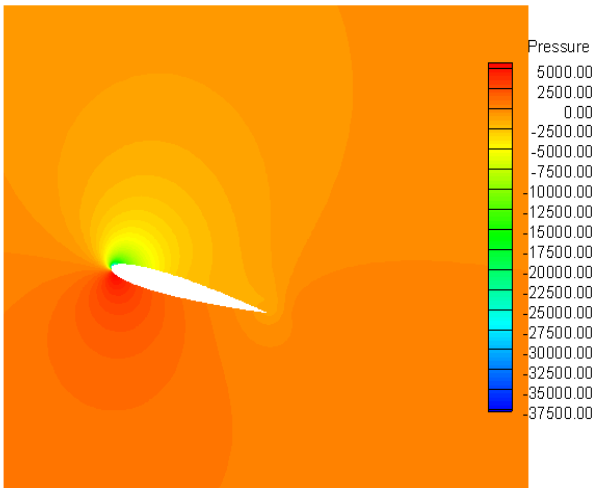
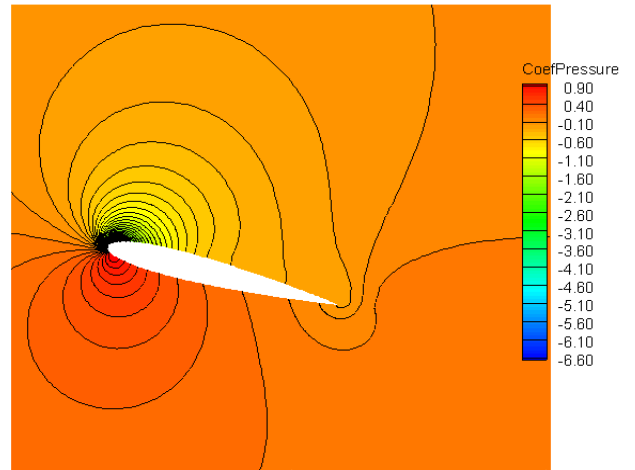
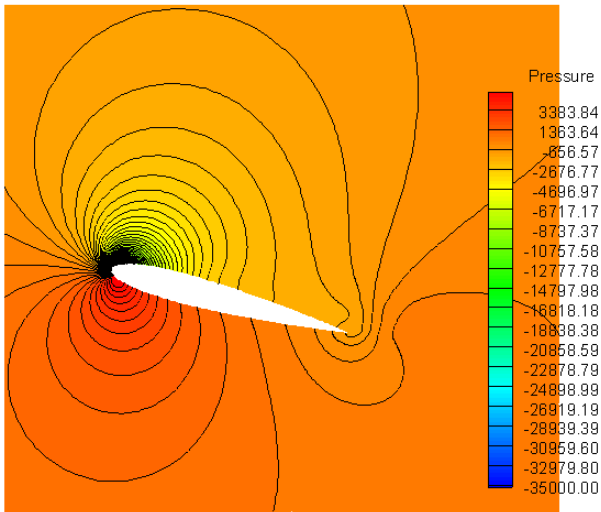
Where t denotes physical-time and τ is a pseudo-time used in the time-marching procedure. If as $\tau \rightarrow \infty$, the second term on the left side of Equation (4) vanishes. The time-dependent term in Equation (4) is discretized in an implicit fashion by means of either a first- or second-order accurate, backward difference in time. The dual-time formulation is written in semi-discrete form as follows which is second order accurate for these simulations:

$$\left[\frac{\Gamma}{\Delta \tau} + \frac{\varepsilon_0 \partial W}{\Delta t \partial Q} \right] \Delta Q^{k+1} + \frac{1}{V} \oint [F - G] \cdot dA = H - \frac{1}{\Delta t} (\varepsilon_0 W^k - \varepsilon_1 W^n + \varepsilon_2 W^{n-1}) \quad (6)$$

Physical time step Δt is limited only by the level of desired temporal accuracy. The pseudo-time-step $\Delta \tau$ is determined by the CFL condition of the time-marching scheme. Normally physical time step is taken as 0.00001 to 0.001s and 500 time steps are taken for these computations. The convective fluxes are calculated by using AUSM+ and all other equations like turbulence etc are taken as second order accurate.

IV. RESULTS AND DISCUSSION

The test conditions for these simulations are M_∞ is taken as 0.283 and Reynolds number 3.45 millions and the convergence criteria for these simulations is taken as for continuity and energy equations is 10^{-6} and for x, y, z velocities and others quantities 10^{-5} to 10^{-6} . For turbulent model the steady state simulations are performed. The unsteady flow calculations are performed for pith up for angle 15° . The airfoil oscillates in pitch about its quarter chord with amplitude of 10° about a 15° mean angle of attack. The residual of the unsteady flow solver is reduced to 10^{-6} from the freestream value. Fig. 5 shows the calculated results in comparison with experimental data[14]. It shows that the results in the up-stroke are in accordance with that of experiment. However, in the down stroke, the results show a qualitative tendency while the separation region is large.



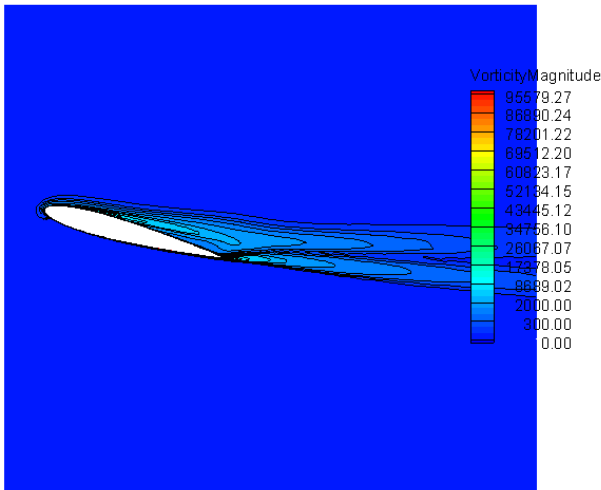


Fig. 2 contours of pressure, absolute pressure, coeff of pressure. Velocity magnitude, stream function and Vorticity magnitude

In figure 2 contours of pressure, absolute pressure, velocity magnitude, stream function and Vorticity magnitude are shown. At the trailing edge and on the upper surface the separated regions are very clear and shown by contours lines.

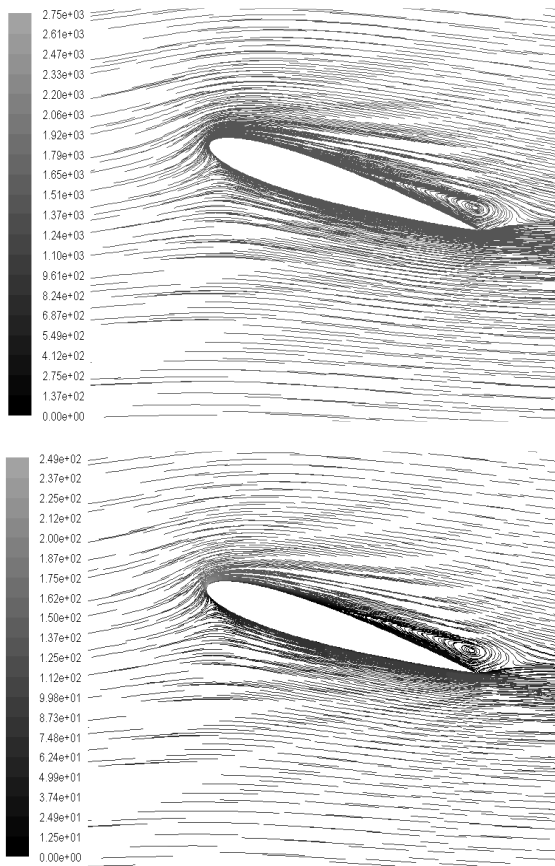


Fig. 3 stream function and velocities magnitude path lines

In figure 3 velocity magnitude and stream function are shown in the form of contours lines the bubble and circulations is clearly shown which are shedding towards the down streams.

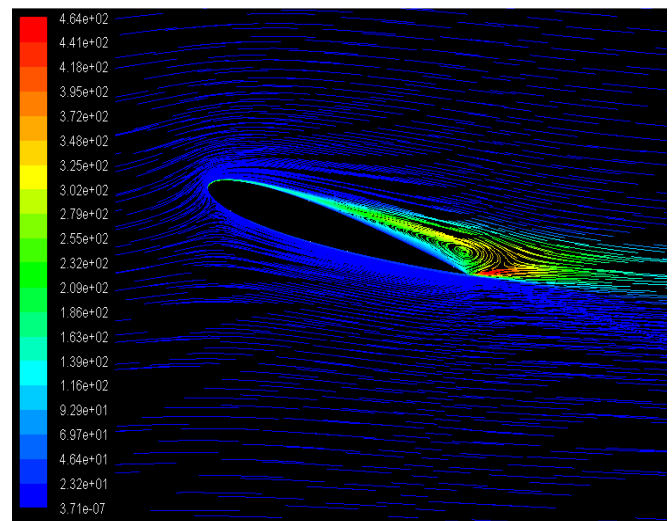
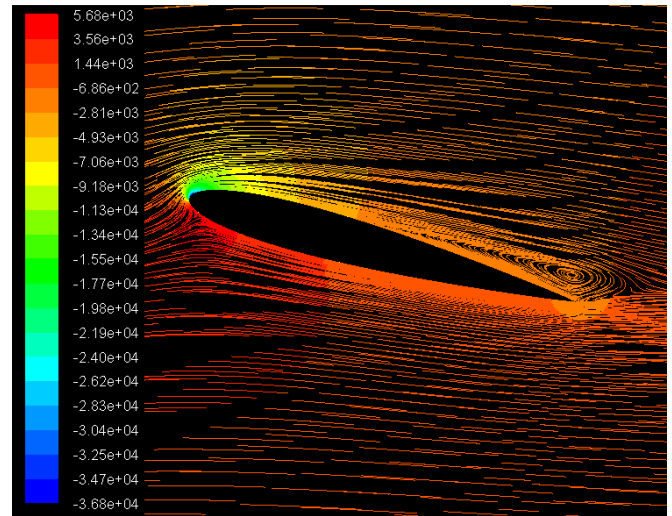


Fig. 4 static pressure and turbulent kinetic energy path lines

In figure 4 static pressure and turbulent kinetic energy path lines are shown. And it is obvious that the turbulence is more in the wake region of the airfoil.

In figure 5 re results of 3 pitch cycle are shown and the results shows how pitching moment, drag and lift coefficients varies during the pitch cycles. The results are same with experimental data during pitch up cycle but have little variations during the returning stroke or down stoke due to large separation regions.

V. CONCLUSION

Unsteady pitch simulations are performed at Mach number .283 by using K- ω SST model and dual time stepping implicit formulations. The results are compared with available data. The Turbulent model resolved the boundary layers and high pressure gradient flows and shows acceptable results in boundary layers and separated region with y^+ value less than 1. During unsteady simulation mesh is dynamics during pitch cycle and it oscillates at .25 of chord. It shows that the results in the up-stroke are in accordance with that of experiment. However, in the down stroke, the results show a qualitative tendency while the separation region is large. In the next research these problems try to be solved to capture the little variation of results during down stroke of the airfoil by chimera meshing.

ACKNOWLEDGMENT

The first author is very thankful to the Pakistan higher Education commission (HEC) for the funding of his PhD and other support to accomplish the project. He is also very thankful to Professor Yan Chao for his kind guidelines for the same.

REFERENCES

- [1] D. G. Mabey, 1999. Unsteady Aero-dynamics: Restrospect and prospect, Aero-nautical Journal, Vol. 103, No. 1019, Review Paper No. 003, 1 - 18.
- [2] W. J. McCroskey, 1982. Unsteady airfoils, Ann. Rev. Fluid Mech., Vol. 14, 285 - 311.
- [3] W. J. McCroskey, 1988. Some Rotorcraft Applications of Computational Fluid Dynamics, NASA TM 100066.
- [4] W. Shyy, M. Berg and D. Lyungvist,, 1999. Flapping and Flexible Wings for Biological and Micro Air Vehicles, Progress in Aerospace Sciences, Vol. 35, No. 5, pp. 455 - 505.
- [5] T. J. Mueller(ed.), 2001. Fixed and Flapping Wing Aerodynamics for Micro Air Vehicles, Progress in Aeronautics and Astronautics, AIAA, Reston, VA, Vol. 195.
- [6] S. Yang, S. Luo and F. Liu, 2006. Optimization of Unstalled Pitching and Plunging Motion of an Airfoil, AIAA paper, submitted to 44th AIAA Aerospace Sciences Meeting and Exhibit, Reno, Nevada, 1055..
- [7] T. Theodorsen, 1934. General theory of aerodynamic instability and the mechanism of flutter, NACA REPORT No. 496.
- [8] I. E. Garrick, 1936. Propulsion of a flapping and oscillating airfoil, NACA Report No. 567.
- [9] I. H. Tuncer and M. F. Platzer, 2000. Computational study of flapping airfoil Aerodynamics, Journal of Aircraft, Vol. 37, pp. 514 - 520.
- [10] K. Isogai, Y. Shinmoto and Y. Watanabe, 1999. Effects of Dynamic Stall on Propulsive Efficiency and Thrust of Flapping Airfoil, AIAA Journal, Vol. 37, pp. 1145 - 1151.
- [11] Ramamurti, R. and Sandberg, W., 2001. Simulation of Flow about Flapping Airfoils using Finite Element Incompressible Flow Solver, AIAA Journal, Vol. 39, pp. 253 - 260.
- [12] J. M. Anderson, K. Streitlien, D. S. Barrett and M.S. Triantafyllou, 1998. Oscillating foils of high propulsive efficiency, J. Fluid Mech., 360, pp. 41 - 72.
- [13] K. Siva Kumar, Sharanappa V. Sajjan " Unsteady Flow past a Combined Pitching and Plunging Aerofoil using an Implicit RANS Solver 2011 International Conference on Mechanical and Aerospace Engineering (CMAE 2011)
- [14] R. I. Issa. Solution of Implicitly Discretized Fluid Flow Equations by Operator Splitting. *J. Comput. Phys.*, 62:40-65, 1986

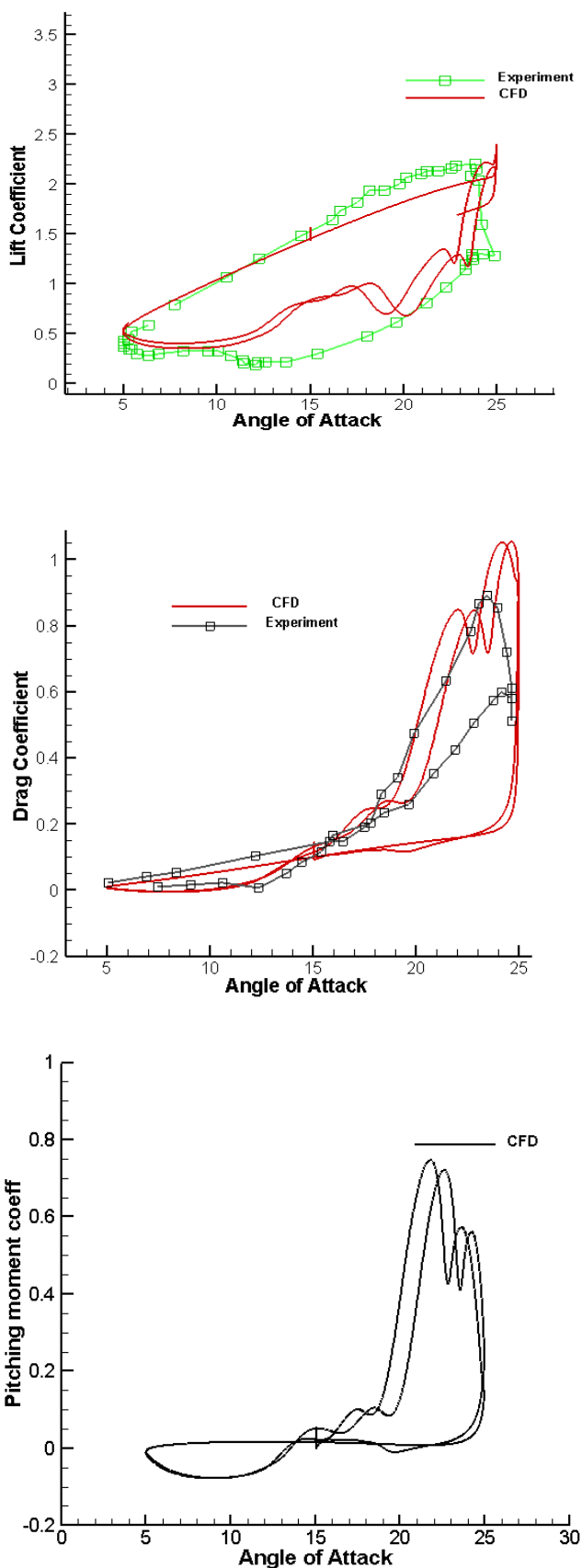


Fig. 5 Drag, lift and pitching moment coefficients v angle of attack for cone-cylinder frustum 5° configuration